Electronic Supplementary Material (ESI) for ChemComm.

Electronic Supplementary information (ESI)

For

Photochemical and electrochemical hydrogen evolution reactivity of lanthanide-functionalized polyoxotungstates

Marzieh Arab Fashapoyeh,[a,b] Masoud Mirzaei, [a]* Hossein Eshtiagh-Hosseini,[a] Ashwene Rajagopal,[b] Manuel Lechner,[b] Rongji Liu[b,c] and Carsten Streb[b]*

[a]Department of Chemistry, Faculty of Science, Ferdowsi University of Mashhad, Mashhad, Iran
[b]Institute of Inorganic Chemistry I, Ulm University, Albert-Einstein-Allee 11, 89081,Ulm, Germany
[c]Key Laboratory of Green Process and Engineering, Institute of Process Engineering, Chinese Academy of Sciences, 100190, Beijing, China

Table of Contents

UV-Vis spectroscopy: UV-Vis spectroscopy was performed on a Shimadzu UV-2450 spectrophotometer, Varian Cary 50 spectrophotometer or Varian Cary 5G spectrophotometer. All systems were used with standard cuvettes (d = 10.0 mm).

X-ray diffraction: Single-crystal X-ray diffraction studies were performed on a Bruker D8 Quest single-crystal diffractometer with a PHOTON II detector using a Mo-Kα radiation (wavelength $\lambda = 0.71073$ Å).

Gas chromatography: Gas-chromatography was performed on a Bruker Scion GC/MS, with a thermal conductivity detector 15 (column: molecular sieve 5A 75 m × 0.53 mm, oven temperature 70 °C, flow rate 25 ml min^{-1}, detector temperature 200 °C) with Argon as a carrier gas. The GC was calibrated by direct injection of known amounts of H_2 gas.

Scanning electron microscopy / energy dispersive X-ray spectroscopy (SEM-EDX): SEM was performed on a Zeiss DSM 962 electron microscope in combination with an EDAX EDS unit for energy dispersive X-Ray spectroscopy. The samples were mounted on carbon tabs and sputtered with carbon before the measurement. SEM studies were performed at an acceleration voltage of 5 kV. EDX measurements were performed at an acceleration voltage of 10 kV.

FT-IR spectroscopy: FT-IR spectroscopy was performed on a Shimadzu IR Prestige-21 FTIR spectrophotometer with a Golden Gate ATR unit. Signals are given as wavenumbers in cm^{-1} using the following abbreviations: vs = very strong, s = strong, m = medium, w = weak and b = broad.

Thermogravimetric (TG): TG analyses were conducted on Mettler–Toledo TGA/SDTA 851e instrument with a heating rate of 10 ^{o}C / min in the temperature range of 25−1000 ^{o}C under a flowing N_2 atmosphere.

Elemental analysis: Elemental analysis was performed on a Euro Vector Euro EA 3000 Elemental Analyzer.

General remarks: All chemicals were purchased from Sigma Aldrich, ABCR or ACROS and were of reagent grade. The chemicals were used without further purification unless stated otherwise.

2. Synthetic section

2.1. Synthesis of {LaW_{11}}

A mixture of $K_8[SiW_{11}O_{39}]$ (1284.8 mg, 0.1 mmol), 3,4-H_2pdc (166.8 mg, 0.25 mmol), $La(NO_3)_3{\cdot}6H_2O$ (433 mg, 0.25 mmol), and H_2O (40 ml) were stirred for 1 h in air. The pH value was adjusted to pH 7 by aqueous NaOH (1 M). The mixture was transferred and sealed in Teflon- lined autoclave and kept at 130 °C for 5 days. After cooling to room temperature, colourless sheet-like crystals of $K_6La[(pdc)_2La(H_2O)_2SiW_{11}O_{39}]$ x *ca.* 15 H_2O were collected after filtration in 65% yield (based on W). The amount of lattice water was determined by thermogravimetric analysis based on the weight loss between room temperature and 150 ^oC.
Elemental analysis for $C_{14}K_{4.5}La_2N_2O_{63.5}SiW_{11}$ in wt.-% (calcd.): C 4.20 (4.40), H 1.07 (1.05), N 0.98 (0.74).

FT-IR spectroscopy (in cm^{-1}): 1650 (m), 1320 (m), 984 (s), 954 (m), 880 (m), 800 (s), 725 (m), 625 (sh).

2.2. Synthesis of {PrW_{11}}

A mixture of $K_8[SiW_{11}O_{39}]$ (1284.8 mg, 0.1 mmol), 3,4-H_2pdc (166.8 mg, 0.25 mmol), $Pr(NO_3)_3{\cdot}H_2O$ (326.9 mg, 0.25 mmol), and H_2O (40 ml) were stirred for 1 h in air. The pH value was adjusted to pH 7 by aqueous NaOH (1 M). The mixture was transferred and sealed in Teflon- lined autoclave and kept at 130 °C for 5 days. After cooling to room temperature, green plate-like crystals of $K_6Pr[(pdc)_2Pr(H_2O)_2SiW_{11}O_{39}]$ x *ca.* 11 H_2O were collected after filtration in 54% yield (based on W). The amount of lattice water was determined by thermogravimetric analysis based on the weight loss between room temperature and 145 ^oC.

Elemental analysis for $C_{14}K_4N_2O_{63.75}Pr_2SiW_{11}$ in wt.-% (calcd.): C 4.31 (4.47), H 0.88 (0.86), N 1.16 (0.74).

FT-IR spectroscopy (in cm^{-1}): 1648 (m), 1322 (s), 980 (s), 953 (m), 878 (s), 798 (m), 730 (m), 620 (w).

2.3. Synthesis of {DyW_{11}}

A mixture of $K_8[SiW_{11}O_{39}]$ (1284.8 mg, 0.1 mmol), 3,4-H_2pdc (166.8 mg, 0.25 mmol), $Dy(NO_3)_3{\cdot}6H_2O$ (438.4 mg, 0.25 mmol), and H_2O (40 ml) were stirred for 1 h in air. The pH value was adjusted to pH 7 by aqueous NaOH (1 M). The mixture was transferred and sealed in Teflon- lined autoclave and kept at 130 °C for 5 days. After cooling to rt, colourless sheet-like crystals of $K_6Dy[(pdc)_2Dy(H_2O)_2SiW_{11}O_{39}]$ x *ca.* 10 H_2O were collected after filtration in 37% yield (based on W). The amount of lattice water was determined by thermogravimetric analysis based on the weight loss between room temperature and 155 ^oC.

Elemental analysis for $C_{13}Dy_{1.45}K_6N_2O_{63.75}SiW_{11}$ in wt.-% (calcd.): C 4.47 (4.47), H 1.05 (0.75), N 0.83 (0.75).

FT-IR spectroscopy (in cm^{-1}): 1652 (m), 1318 (vs), 988 (vs), 950 (m), 882 (m), 795 (m), 735 (m), 615 (m).

2.4. Synthesis of POM@rGO composites

In a typical synthesis, an aqueous solution of the respective cluster (**{W_{11}}**, **{LaW_{11}}**, **{PrW_{11}}** or **{DyW_{11}}**) (15 mL, 1.6 mM) in 0.5 M H_2SO_4 (pH = 0.3) was mixed with an aqueous solution of GO (1 mL, 0.6 mg mL^{-1}) under sonication and stirring to form a homogeneous suspension. Controlled potential coulometry measurements were conducted in a three-electrode conventional glass cell with the mixed suspension of POM and GO as the electrolyte solution. A glassy carbon (GC) plate (with surface area of 2 cm^2) was used as the working electrode, a saturated calomel electrode (SCE) was used as the reference electrode and a Pt foil with a large surface area of 3 cm^2 was used as the counter electrode. The electrolyte was saturated with ultrahigh-purity Ar for at least 30 min and kept under a positive pressure of this gas during the experiments. A potential of -1.1 V vs. SCE was set on the working electrode to fully reduce the POM solution by 12 electrons. After the electrochemical reduction was completed, the cell with a dark-blue suspension of POM@rGO was covered tightly and allowed to stand for several hours until the blue color disappeared. Then, the suspension was centrifuged and washed thoroughly with ultrapure water 3 times and ethanol once. Then, the composites were dried in the oven at 80 °C for overnight.

3. Characterization

3.1 Crystallographic information

Single-crystal structure determination: Suitable single crystals of the respective compound were grown and mounted onto the end of a thin glass fibre using Fomblin oil. Single-crystal X-ray diffraction studies were performed at 150 K on Bruker D8 Quest single-crystal diffractometer with a PHOTON II detector using a Mo-Kα radiation (wavelength λ = 0.71073 Å). Structure solution and refinement was carried out using the SHELXL package via Olex2. Corrections for incident and diffracted beam absorption effects were applied using multi-scan. Structures were solved by a combination of direct methods and difference Fourier syntheses and refined against F^2 by the full-matrix least-squares technique. During refinement, parts of the molecules were modelled with restraints or isotropically due to significant disorder. Several datasets were recorded for each crystal type and the best data sets are reported here. Crystal data, data collection parameters and refinement statistics are listed in Tables S1-3.

Table S1. Summary of the crystallographic information for **{LaW$_{11}$}**.

CCDC no	1857778
Empirical formula	$C_{14}K_{4.5}La_2N_2O_{63.5}SiW_{11}$
Formula weight	3716.37
Temperature/K	150.0
Crystal system	Monoclinic p
Space group	P 1 21/n 1
a/Å	11.5296 (10)
b/Å	30.702 (3)
c/Å	17.9958 (14)
α/°	90
β/°	101.940 (3)
γ/°	90
Volume/Å^3	6232.3 (9)
Z	4
ρ_{calc}g/cm^3	3.961
μ/mm^{-1}	21.995
F(000)	6534
Crystal size/mm^3	0.04 × 0.12 × 0.14
Radiation	MoKα (λ = 0.71073)
2Θ range for data collection/°	7.028 to 52.744
Index ranges	$-19 \le h \le 14$, $-51 \le k \le 38$, $-30 \le l \le 22$
Reflections collected	111512
Independent reflections	12731 [R_{int} = 0.0488, R_{sigma} = 0.0244]
Data/restraints/parameters	12731/6/886
Goodness-of-fit on F^2	1.083
Final R indexes [I>=2σ (I)]	R_1 = 0.0259, wR_2 = 0.0579
Final R indexes [all data]	R_1 = 0.0292, wR_2 = 0.0593
Largest diff. peak/hole / e Å^{-3}	3.55/-2.73

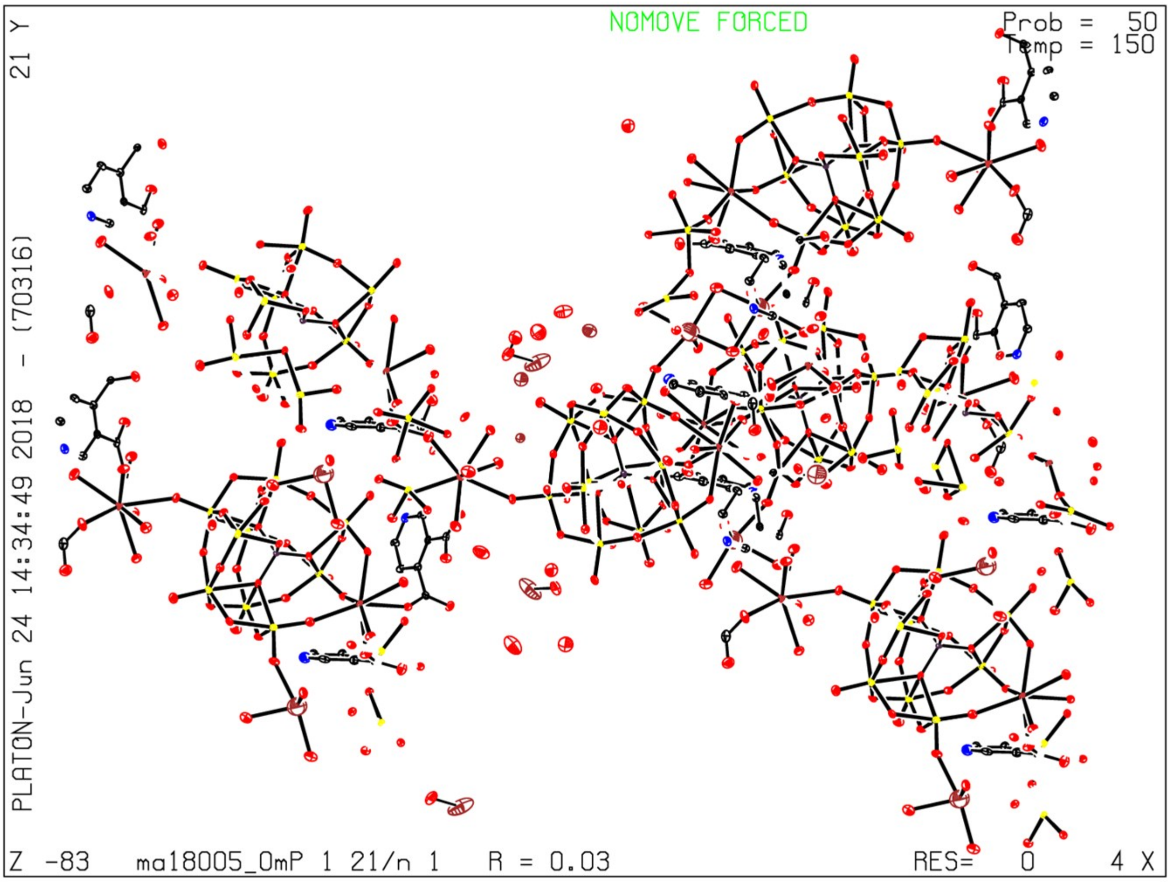

Figure S1: ORTEP representation of **{LaW$_{11}$}**, probability ellipsoids given at 50 %.

Table S2. Summary of the crystallographic information for **{DyW$_{11}$}**.

CCDC no	1857777
Empirical formula	$C_{13}Dy_2K_6N_2O_{64}SiW_{11}$
Formula weight	3714.81
Temperature/K	150.0
Crystal system	Monoclinic p
Space group	P 1 21 1
a/Å	10.6779 (5)
b/Å	20.1665 (9)
c/Å	15.5021 (8)
α/°	90
β/°	103.3465 (19)
γ/°	90
Volume/Å^3	3248 (3)
Z	2
ρ_{calc}g/cm^3	3.809
μ/mm^{-1}	21.561
F(000)	3279
Crystal size/mm^3	0.118 × 0.156 × 0.2
Radiation	MoKα (λ = 0.71073)
2Θ range for data collection/°	7.015 to 51.360
Index ranges	$-17 \le h \le 12$, $-33 \le k \le 24$, $-25 \le l \le 18$
Reflections collected	130900
Independent reflections	70843 [R_{int} = 0.0575, R_{sigma} = 0.0383]
Data/restraints/parameters	12297/67/448
Goodness-of-fit on F^2	1.0750
Final R indexes [I>=2σ (I)]	R_1 = 0.0262, wR_2 = 0.0633
Final R indexes [all data]	R_1 = 0.0291, wR_2 = 0.0652
Largest diff. peak/hole / e Å^{-3}	1.84/-2.92

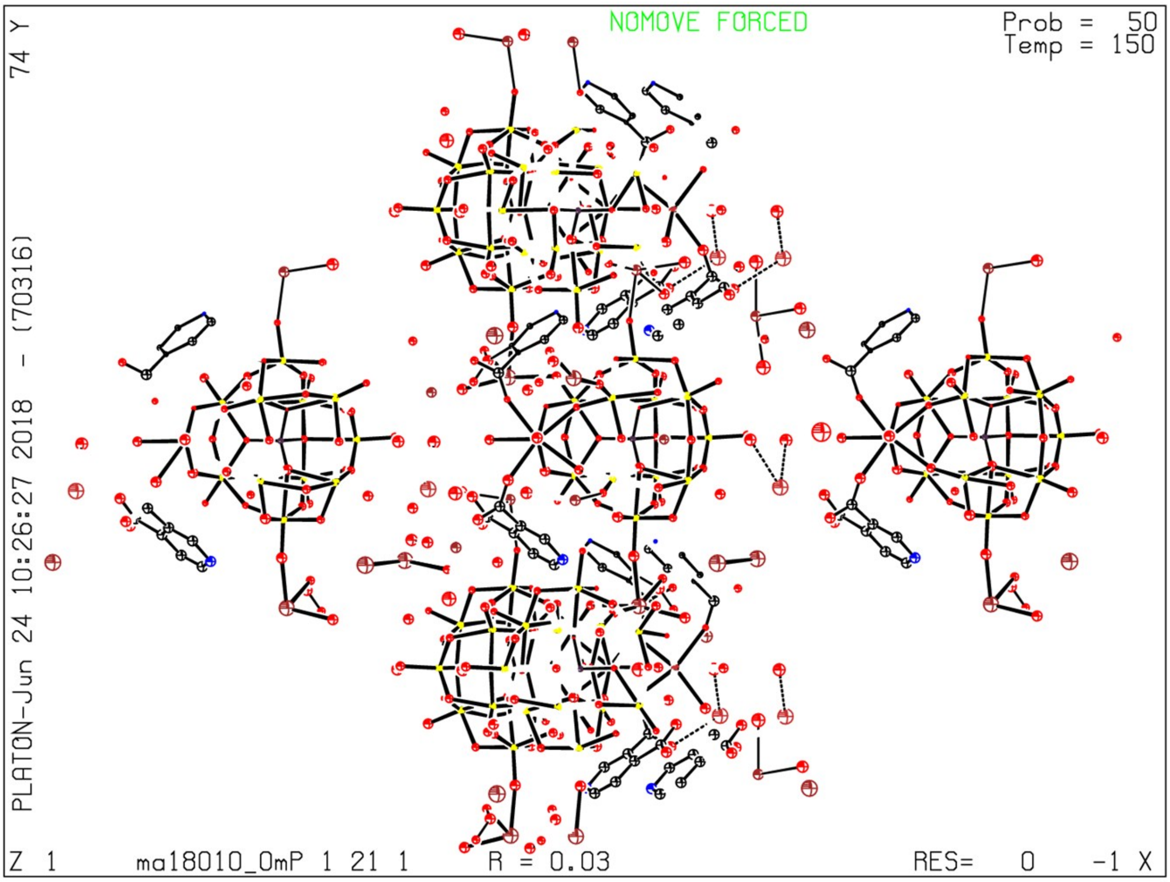

Figure S2: ORTEP representation of **{DyW$_{11}$},** probability ellipsoids given at 50 %.

Table S3. Summary of the crystallographic information for **{PrW$_{11}$}**.

CCDC no	1857779
Empirical formula	$C_{14}K_4N_2O_{64}Pr_2SiW_{11}$
Formula weight	3704.82
Temperature/K	150.0
Crystal system	Monoclinic p
Space group	P 1 21/n 1
a/Å	11.4529 (13)
b/Å	30.495 (3)
c/Å	17.907 (2)
α/°	90
β/°	101.994 (4)
γ/°	90
Volume/Å^3	6117.5 (12)
Z	4
ρ_{calc}g/cm^3	4.023
μ/mm^{-1}	22.570
F(000)	6520
Crystal size/mm^3	0.04 × 0.057 × 0.155
Radiation	MoKα (λ = 0.71073)
2Θ range for data collection/°	7.074 to 51.364
Index ranges	$-14 \leq h \leq 13$, $-38 \leq k \leq 37$, $-22 \leq l \leq 21$
Reflections collected	110386
Independent reflections	102527 [R_{int} = 0.1495, R_{sigma} = 0.0707]
Data/restraints/parameters	11556/0/458
Goodness-of-fit on F^2	1.1480
Final R indexes [I>=2σ (I)]	R_1 = 0.0846, wR_2 = 0.2064
Final R indexes [all data]	R_1 = 0.1066, wR_2 = 0.2249
Largest diff. peak/hole / e Å^{-3}	4.26/-4.23

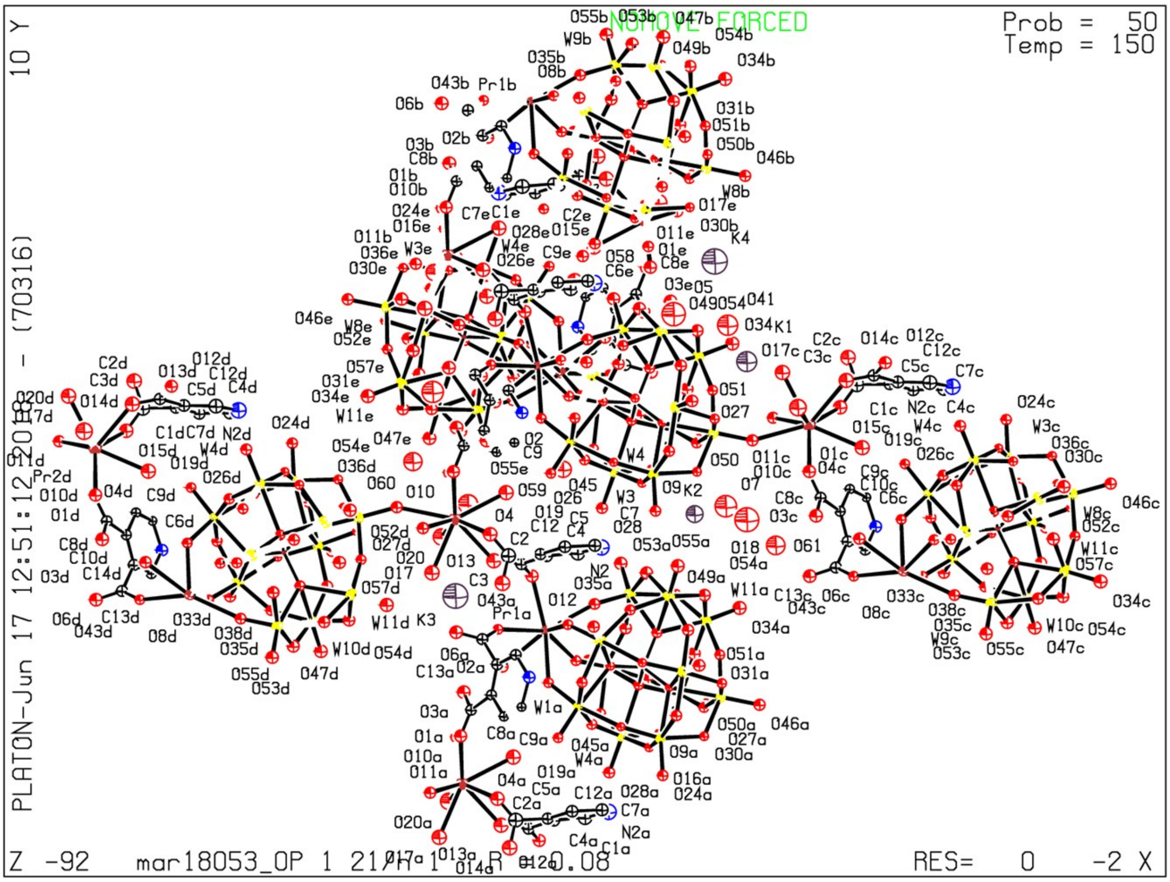

Figure S3: ORTEP representation of **{PrW$_{11}$}**, probability ellipsoids given at 50 %.

4. Light-driven hydrogen evolution experiments

Experiments were carried out in 21 mL Schlenk-tubes filled with 8 mL of the catalytic solution, capped with rubber septa and placed in custom-built, air-cooled photo-reactors using irradiation by LED arrays (λ= 470 nm).

The gas phase above the solution was probed by inserting a gas-tight GC syringe through the septum, taking a volume of 100 µL of the gas phase and analysing the amount of hydrogen in the gas phase using GC. The GC was calibrated by mixing different volumes of pure hydrogen with argon in a Schlenk-vessel[1]. The injected amount of hydrogen was plotted against the peak area to gain a calibration curve to enable recalculation of peak areas to amounts of hydrogen from catalysis samples.

Control experiments were performed and showed no hydrogen evolution when the samples are not irradiated, or when catalyst**,** $[Ru(bpy)_3]^{2+}$ or ascorbic acid are absent.

4.1. Comparative study on different Keggin-type clusters as photocatalyst for light-driven hydrogen evolution reaction

Table S4. Comparison of the reported catalysts with previously reported POM-HER systems under homogeneous, light-driven conditions

[Catalyst]	[PS]/[Co-Catalyst]	Electron donor / solvent	TON	Irradiation Time (h)	Reference
$[\alpha\text{-}[Al(H_2O)SiW_{11}O_{39}]^{5-}]$, (1.2mM)	[Eosin-Y], 0.2μM/ [Pt], 0.24μM	TEOA/ 1.0M HCl	12.5	20	[2]
$[Na_{10}[Mn_4(H_2O)_2(VW_9O_{34})_2]]$, (22.9μM)	$[[Ru(bpy)_3]^{2+}]$, 0.67mM	TEOA/ $DMF:H_2O$ (1.86:1, v:v)	35	5	[3]
$[K_7[Co^{III}Co^{II}(H_2O)W_{11}O_{39}]]$, (40μM)	[Eosin-Y], 50μM/ [Pt], 5 wt%	TEOA/ H_2O (5%v/v)	100	2.3	[4]
$[[M(H_2O)TiW_{11}O_{39}]^{n-}]$; [M= Fe, Co, Zn], (0.05mM)		PVA/H_2O	3.2 [M= Co]	3	[5]
$[[Ni(H_2O)MW_{11}O_{39}]^{n-}]$; [M= P, SI, Ge], (51μM, M= Ge)	$[[Ru(bpy)_3]^{2+}]$, 1mM	Ascorbate buffer/ H_2O	52 [M= Ge]	15	[6]
$[K_6M[(pdc)_2M(H_2O)_2SiW_{11}O_{39}]]$; [M= La, Dy, Pr], (0.5μM)	$[[Ru(bpy)_3]^{2+}]$, 20μM	Ascorbic Acid/ $H_2O:MeOH$ (9:1, v:v)	525 [M= La]	7	This work

PS = Photosensitizer, ED = electron donor, TEOA = Triethanolamine, bpy = 2,2'-bipyridine, TON = turnover number, DMF = dimethyl formamide.

5. Colloid detection procedure

To exclude the formation of colloidal particles (e.g. by precipitation of $[Ru(bpy)_3]^{2+}$/Keggin cluster salts) in the above reaction system, a literature-known colloid detection procedure[7] using micro-filtration (using a 0.2 μm pore size PTFE syringe filter), UV-Vis spectrometry and scanning electron microscopy / energy-dispersive X-ray spectroscopy was performed. For all samples reported, no colloid formation was observed over the course of the catalytic reaction.

5.1 Micro-filtration of the solutions using a 0.2 μm pore size PTFE syringe filter and UV-Vis spectroscopic analysis of the solutions before and after filtration show no significant change in the UV-Vis spectroscopic trace of the catalyst-containing solutions. **SEM-EDX analysis** of the filter membrane show no particles and do not feature EDX signals for Si, W, La, Dy or Ru, see below.

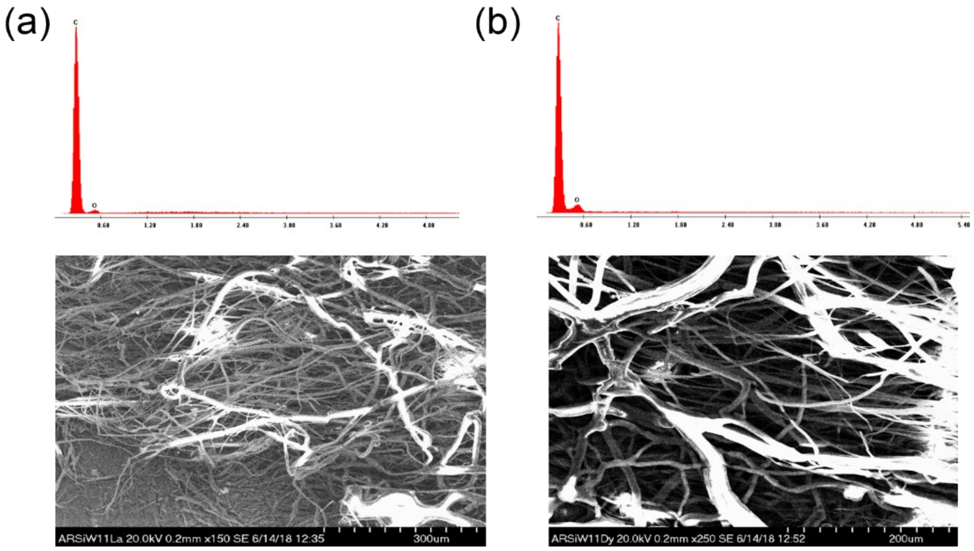

Figure S4: (a) **Top**. EDX analysis of the filter membrane (fibrous structure) after filtration shows that no colloidal particles (no Si, W, La, Ru detected by EDX) are retained on the membrane. **Bottom.** Scanning electron microscopic picture of the filter membrane after filtration of the catalytic solution. (b) **Top.** EDX analysis of the filter membrane (fibrous structure) after filtration shows that no colloidal particles (no Si, W, Dy, Ru detected by EDX) are retained on the membrane. **Bottom.** Scanning electron microscopic SEM picture of the filter membrane after filtration of the catalytic solution.

5.2. UV-Visible Spectroscopy of the catalytic solution before the microfiltration and after microfiltration was performed. This test was done for all the three catalytic solutions and obtained a similar UV-Vis spectrum.

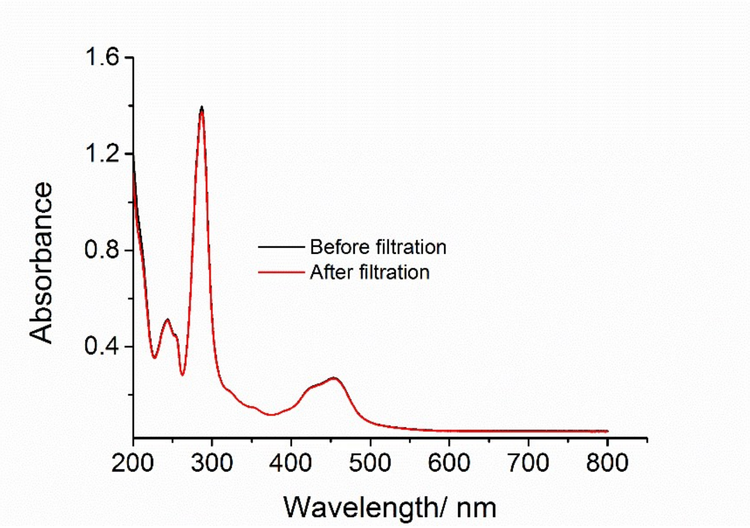

Figure S5: UV-Vis spectroscopic analysis of the reaction solution before and after micro-filtration. No changes are observed after filtration.

5.3 UV-Visible Spectroscopy of the photosensitizer degradation after 6h catalytic reaction:

The catalytic reactions were continued for 6h only as a degradation of the photosensitizer $[Ru(bpy)_3]^{2+}$ was observed within this span of time. A UV-Visible spectroscopy could show the deviation in the absorbance of the photosensitizer before and after the irradiation time.

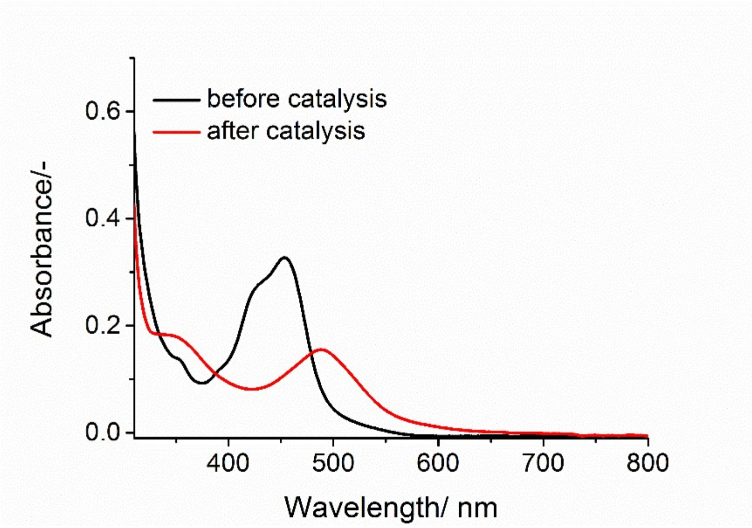

Figure S6: UV-Vis spectroscopic analysis of the catalytic solution before irradiation and after 6h of irradiation.

5.4. Proposed simplified scheme of light-driven HER by {LnW$_{11}$}

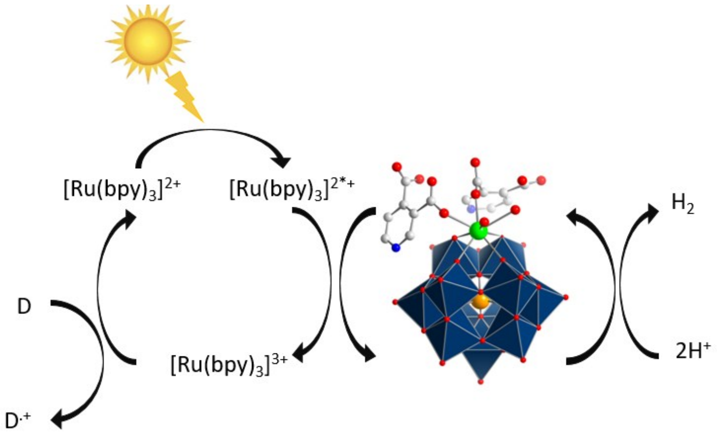

Figure S7: proposed mechanism of light-driven HER by **{*Ln*W$_{11}$}** based on electron transfer from the photosensitizer to the catalyst and subsequent regeneration of the photosensitizer by the sacrificial electron donor D.

6. Electrocatalytic hydrogen evolution reaction (HER)

Preparation of the modified electrodes. Typically, 1 mg of the finely ground **POM@rGO** (**{W$_{11}$}@rGO**, **{LaW$_{11}$}@rGO**, **{PrW$_{11}$}@rGO** or **{DyW$_{11}$}@rGO**) was dispersed in 0.2 mL of anhydrous alcohol (5 mg mL^{-1}) by at least 1 h sonication to form a homogeneous ink. Then, 7.5 µL of the catalyst ink was loaded onto a glassy carbon rotating disk electrode (RDE) of 4 mm diameter (the loading of catalysts was 0.3 mg cm^{-2}). After drying, the electrode was further modified with a thin film of Nafion by dropping 1.0 µL of 0.5 wt% Nafion solution (isopropanol as the solvent) onto its surface.

HER measurements. The electrochemical set-up was a CHI 730E electrochemical workstation (CHI Instrument, Inc.). A standard three-electrode cell was used. The prepared thin film modified RDE was used as the working electrode. A graphite rot was used as the counter electrode, and a SCE was used as the reference electrode. The electrolyte, consisting of a solution of 0.5 M H_2SO_4 (pH = 0.3), was saturated with ultrahigh-purity Ar for 30 min before linear sweep voltammetry (LSV) measurements. The SCE was calibrated with respect to the reversible hydrogen electrode (RHE) in all measurements based on the Nernst equation ($E_{RHE} = E_{SCE} + E^0_{SCE} + 0.059$ pH). In 0.5 M H_2SO_4, $E_{RHE} = E_{SCE} + 0.265$ V.

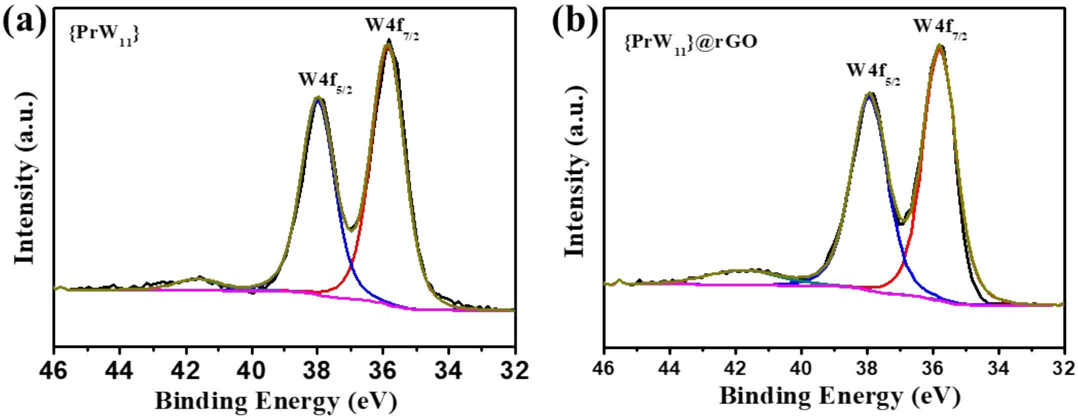

Figure S8: High resolution W 4f XPS spectra for **{PrW$_{11}$}** and **{PrW$_{11}$}**@rGO.

Table S5. The binding energies (BE) of W 4f for {PrW$_{11}$} and {PrW$_{11}$}@rGO.

Samples	BE (W 4f$_{7/2}$) / eV	BE (W 4f$_{5/2}$) / eV
{PrW$_{11}$}	35.87	38.00
{PrW$_{11}$}@rGO	35.79	37.94

Fig. S8 shows the high resolution W 4f XPS spectra for **{PrW$_{11}$}** and **{PrW$_{11}$}**@rGO. Slightly lower W binding energies are noted for the composite compared with the native **{PrW$_{11}$}** (Table S5), indicating that significant interactions between catalyst and substrate could be present which could affect the HER activity of the catalyst.

7. Literature

1 S. Rau, B. Schäfer, D. Gleich, E. Anders, M. Rudolph, M. Friedrich, H. Görls, W. Henry and J. G. Vos, *Angew. Chemie - Int. Ed.*, 2006, **45**, 6215–6218.

2 X. Liu, Y. Li, S. Peng, G. Lu and S. Li, *Int. J. Hydrogen Energy*, 2012, **37**, 12150–12157.

3 H. Lv, J. Song, H. Zhu, Y. V Geletii, J. Bacsa, C. Zhao, T. Lian, D. G. Musaev and C. L. Hill, *J. Catal.*, 2013, **307**, 48–54.

4 J. Zhao, Y. Ding, J. Wei, X. Du, Y. Yu and R. Han, *Int. J. Hydrogen Energy*, 2014, **39**, 18908–18918.

5 X. Shang, R. Liu, G. Zhang, S. Zhang, H. Cao and Z. Gu, *New.J.Chem*, 2014, **40**, 1315–1320.

6 K. Von Allmen, R. Morø, R. Müller, J. Soriano-lópez, A. Linden and G. R. Patzke, *Chempluschem*, 2015, **80**, 1389–1398.

7 B. Kirchhoff, C. Streb, S. Rau and C. Streb, *Eur. J. Inorg. Chem.*, 2016, **2016**, 1425–1429.